doi: 10.17221/56/2013-RAE

Mathematical and neural network modelling of terebinth fruit under fluidized bed drying

M. Kaveh, R. Amiri Chayjan

Department of Biosystems Engineering, Faculty of Agriculture, Bu-Ali Sina University, Hamedan, Iran

Abstract

Kaveh M., Chayjan R.A. (2015): **Mathematical and neural network modelling of terebinth fruit under fluidized bed drying**. Res. Agr. Eng., 62: 55–65.

The paper presents an application which uses Feed Forward Neural Networks (FFNNs) to model the non-linear behaviour of the terebinth fruit drying. Mathematical models and Artificial Neural Networks (ANNs) were used for prediction of effective moisture diffusivity, specific energy consumption, shrinkage, drying rate and moisture ratio in terebinth fruit. Feed Forward Neural Network (FFBP) and Cascade Forward Neural Network (CFNN) as well as training algorithms of Levenberg-Marquardt (LM) and Bayesian regularization (BR) were used. Air temperature and velocity limits were 40–80°C and 0.81–4.35 m/s, respectively. The best outcome for the use of ANN for the effective moisture diffusivity appertained to CFNN network with BR training algorithm, topology of 2-3-1 and threshold function of TANSIG. Similarly, the best outcome for the use of ANN for drying rate and moisture ratio also appertained to CFNN network with LM training algorithm, topology of 3-2-4-2 and threshold function of TANSIG.

Keywords: MLP; moisture diffusivity; drying rate; shrinkage; multi-layer perceptron

Terebinth (*Pistacia atlantica* L.) is an ancient and long-life tree with about 5 m height. Terebinth fruit is small and spherical-like with dark green colour. Kernel of terebinth fruit is similar to pistachio, but much smaller. Terebinth fruit is used in buttermilk process and animal oils and also it is used to make pickles. The harvested terebinth fruit has too much moisture (about 2.6 g H_2O/g of dry matter (d.m.)), which causes fast spoilage of the fruit.

Drying is defined as a preservation method applied at industrial scale in order to minimize the biochemical, chemical, and microbiological spoilage by reducing the water quantity and the water activity of fruits and vegetables. Water is transferred by diffusion from the interior of food material to the air-food interface and from there to the air stream by convection (Cakmak, Yildiz 2011).

Fluidized bed drying is one of the best methods in dehydration of high moisture products. This method can improve the quality of final product, such as: colour, taste and nutritional content (Alibas 2007). Moreover, this method can increase the moisture removal rate. Fluidization includes minimum fluidized bed (semi-fluidized bed) and bubbling fluidized bed. Fixed bed is before minimum fluidized bed and transportation phenomenon occurs after bubbling fluidized bed (Amiri Chayjan et al. 2012).

In practical applications drying process requires high energy input because of high latent heat of water evaporation and relatively low energy efficiency of industrial dryers. Thus, one of the most important challenges of the industrial dryers is to reduce the energy cost versus good quality of dried products (Nazghelichi et al. 2011).

doi: 10.17221/56/2013-RAE

Effective moisture diffusivity (D_{eff}) is an important index in modelling, designing and optimizing of a drying process. Effective moisture diffusivity value determines the mass transfer rate from product in drying process (Hashemi et al. 2009).

One of the undesirable changes which occur simultaneously within moisture diffusion in drying process is the reduction of volume or shrinkage; modifying physical properties, heat and mass exchange area and in particular affecting the diffusion coefficient of the materials. In general, shrinkage occurs as a result of volume reduction due to evaporation of the moisture contained in the solid. Heating and loss of water cause stresses in the cellular structure of the food and lead to changes in shape and decrease in dimensions (Mayor, Sereno 2004; Hashemi et al. 2009).

An artificial neural network (ANN) consists of processor units, namely neurons, which are connected with each other in special arrangement. Every network includes some neurons in the input layer and in one or more hidden layers, and also one or more neurons in the output layer. Variations in neuron model and relationship between neurons, and their weights determine algorithms and architectures of ANN. ANN has powerful learning ability and identifying and modelling ability for the complex non-linear relationships between the input and the output of a system (Nazghelichi et al. 2011). Some workers applied ANNs for modelling of drying (Bala et al. 2005; Movagharnejad, Nikzad 2007; Lertworasirikul, Tipsuwan 2008; Amiri Chayjan et al. 2012).

No study has been reported about moisture diffusivity, shrinkage, specific energy consumption*s*, drying rate and moisture ratio of terebinth fruit by ANN method. The main goals of this study were artificial neural network modelling of effective moisture diffusivity, specific energy consumption, shrinkage, drying rate and moisture ratio of terebinth fruit.

MATERIAL AND METHODS

Fresh terebinth (*Pistacia atlantica* L.) was harvested from the Sardasht forests in Iran and stored in a refrigerator at about 4°C. The initial moisture content of the terebinth was determined by drying of 30 g of sample in an oven at 70 ± 1°C. Experiments were replicated three times. The initial moisture content of the terebinth was observed to be 2.6 g H_2O/g d.m. The drying of terebinth fruit was investigated in a laboratory scale fluidized bed dryer (FBD) developed in the Bu-Ali Sina University, Hamedan, Iran (Amiri Chayjan, Kaveh 2014).

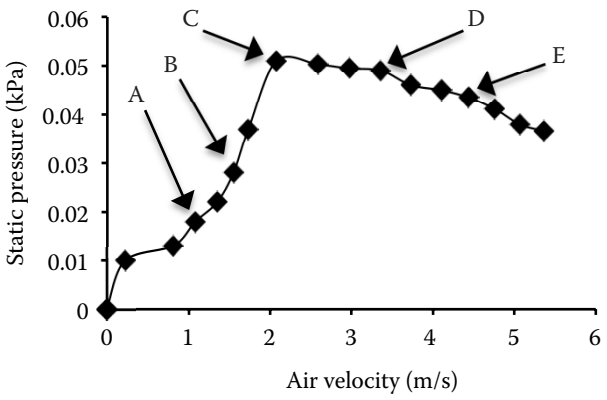

Fig. 1. Fluidization curve of terebinth fruit and selected points for modelling

A, B – fixed bed (0.81 and 1.38 m/s); C – semi fluid bed (2.08 m/s); D, E – fluid bed (3.35 and 4.43 m/s)

Five experimental points of drying were selected on fluidization curve (Fig. 1). At first, pressure drop of terebinth was determined at different air flow velocities. Fan speed was gradually increased using an inverter (Vincker VSD2; ABB Co., Taipei, Taiwan) and parameters of pressure drop and air velocity were recorded using a multifunction measurement device (Standard ST-8897; Standard Instruments Co., Kowloon, Hong Kong). It consists in a differential digital manometer with ± 0.1 Pa accuracy and a vane type digital anemometer with ± 0.1 m/s accuracy (Lutron AM-4202; Electronic Enterprise Co., Taipei, Taiwan). Max. value of static pressure drop (point C in Fig. 1) in fluidization curve of terebinth is known as min. fluidization point or semi fluidized bed. Experimental points in fixed bed domain were determined with air velocities about 0.81 and 1.35 m/s (points A and B in Fig. 1), also experimental points D and E with air velocities about 3.35 and 4.43 m/s, respectively, was selected as a fluidized bed condition. Five bed conditions (fixed bed at 0.81 and 1.35 m/s, semi fluidized bed at 2.08 m/s and fluidized bed at 3.35 and 4.43 m/s) and five air temperatures of 40, 50, 60, 70 and 80°C were applied in the drying experiments. Drying experiments were conducted in three replications.

Fick's second low of diffusion with sphere geometry was used for computing the effective moisture

doi: 10.17221/56/2013-RAE

diffusivity. It was assumed that seed shrinkage after drying process is negligible and distribution of initial moisture is uniform. Fick's equation for computing effective moisture diffusivity of terebinth seeds is as follows:

$$\ln(MR) = \ln\left(\frac{M_t - M_e}{M_0 - M_e}\right) = \ln\left(\frac{6}{\pi^2}\right) - \left(\frac{D_{\text{eff}}\pi^2 t}{r^2}\right) \quad (1)$$

where:

MR – moisture ratio

M_t – moisture content at any time (% d.b.)

M_e – equilibrium moisture content (% d.b.)

M_0 – initial moisture content (% d.b.)

n – number of terms taken into consideration

t – drying time (s)

D_{eff} – effective moisture diffusivity (m^2/s)

r – radius of kernel (m)

Specific energy consumption (*SEC*) for terebinth drying was obtained using the thermodynamic models (Amiri Chayjan, Kaveh 2014).

Ten terebinth fruits were used for each shrinkage measurement. Shrinkage was expressed in terms of the percentage change of the volume of terebinth as compared with its original volume:

$$S_b = \frac{\left(V_0 - V_f\right)}{V_0} \times 100 \quad (2)$$

where:

S_b – shrinkage (%)

V_0 – volumes of terebintht the beginning (before drying)

V_f – volumes of terebinth at the end of each boiling experiment

The measurement of the sample volume was performed using a digital calliper (SKU 8372062; Pro Tool Point Inc., Lake Forest, USA) (Niamnuy et al. 2012).

The drying rate is approximately proportional to the difference in moisture content between the material being dried and equilibrium moisture content at the drying air state (Cakmak, Yaldiz 2011). According to this definition, the drying rate (*DR*) of terebinth samples is usually determined using:

$$DR = \frac{\left(M_{t+dt} - M_t\right)}{dt} \quad (3)$$

where:

M_t – moisture content at any time (% d.b.)

t – drying time (min)

The most common types of ANN are Feed and Cascade forward neural networks. These networks are applied to predict outputs of new unknown patterns. Furthermore, in this study, these networks as well as two learning algorithms were utilized. Feed Forward Back Propagation (FFBP) consists of input, hidden and output layers (Amiri Chayjan, Esna-Ashari 2010). Back propagation (BP) learning algorithm was used to train this network. During training by BP algorithm, layer weights were updated at the first epoch. The weight coefficients were updated by learning rules and weight values. During training this network, calculations were conducted from input to output and error values were then propagated to prior layers. Cascade Forward Back Propagation (CFBP) operation using the BP algorithm for weights updating is similar to FFBP network, but the main feature of this network is that each layer of neurons is connected to all previous neurons layers. Two algorithms including Levenberg-Marquardt (LM) and Bayesian regulation (BR) back propagation algorithms were used for network training (Keeratipibul et al. 2011).

Applying the two inputs in all experiments, the effective moisture diffusivity, specific energy consumption and shrinkage values were calculated for different conditions. In the first type networks, two neurons in input layer (air velocity and temperature) and one neuron in output layer (D_{eff}, *SEC* or shrinkage) were considered. Also with applying three inputs (air velocity, air temperature and drying time) in all experiments, the *DR* and *MR* values were computed for different conditions.

Figs 2 and 3 show the input and output parameters for considered neural network topologies. Levels and boundaries of input parameters are presented in Table 1. Matlab software (The MathWorks Inc., Natick, USA) with neural network toolbox was used in this study.

Table 1. Input parameters for artificial neural networks and their boundaries for prediction of effective moisture diffusivity, specific energy consumption and shrinkage of terebinth, drying rate and moisture ratio of terebinth

Parameter	Min.	Max.	No. of levels
Air temperature (°C)	40	80	5
Air velocity (m/s)	0.81	4.43	5
Time (min)	3	420	147

doi: 10.17221/56/2013-RAE

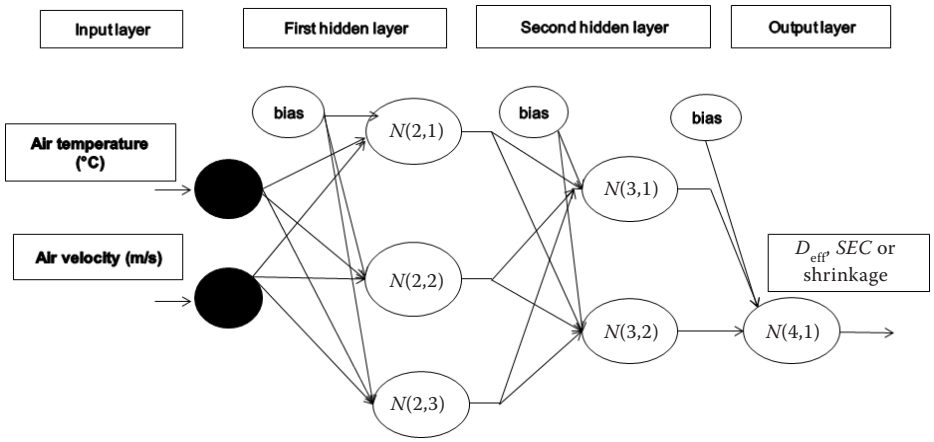

Fig. 2. Artificial neural network topology of D_{eff}, *SEC* or shrinkage of terebinth fruit
N – number of neurons; D_{eff} – effective moisture diffusivity; *SEC* – specific energy consumption

Optimized number of layers and neurons for various topologies was selected by increasing method. With this approach, when the output was trapped into the local minimum, new neuron and layer were gradually added to the network. Also different threshold functions were tested to achieve the optimized topology (Demuth et al. 2007):

$$Y_j = X_i \quad \text{(PURELIN)} \tag{4}$$

$$Y_j = \frac{2}{\left(1+\exp(-2X_j)\right)-1} \quad \text{(TANSIG)} \tag{5}$$

$$Y_j = \frac{1}{1+\exp\left(-X_j\right)} \quad \text{(LOGSIG)} \tag{6}$$

where:
Y_j – j^{th} neuron output
X_j – sum of weighed inputs for each neuron in j^{th} layer and computed according to Eq. (7):

$$X_j = \sum_{i=1}^{m} W_{ij} \times Y_i + b_j \tag{7}$$

where:
m – number of output layer neurons
W_{ij} – weight coefficient between i^{th} and j^{th} layers
Y_i – i^{th} neuron output
b_j – bias of j^{th} neuron for FFBP and CFBP networks

Experimental data of 40, 50, 60, 70 and 80°C were selected for training network with suitable topology and training algorithm. About 75% of all data were randomly selected for training network with suitable topology and training algorithm.

The index of mean square error (*MSE*) is determined to minimize the training error (Demuth et al. 2007). Also the supplementary indices of determination coefficient (R^2), root mean square error, mean absolute error (*MAE*) and standard er-

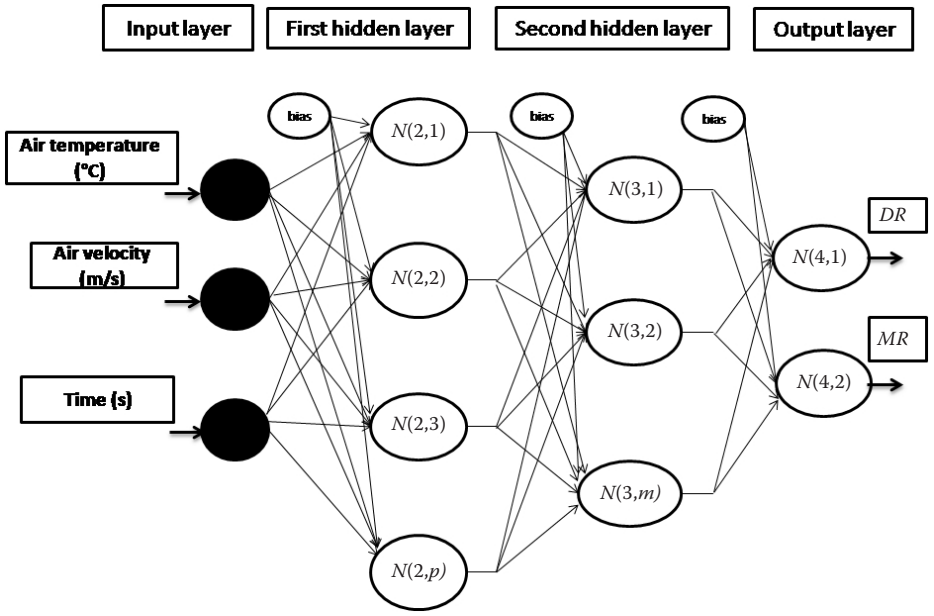

Fig. 3. Artificial neural network topology of *DR* and *MR* of terebinth fruit
DR – drying rate; *MR* – moisture ratio, *N* – number of neurons; *p* – number of neurons in the layer; *m* – number of output layer neurons

doi: 10.17221/56/2013-RAE

ror (STD_{MAE}) were used to optimize the network from prior stage (Amiri Chayjan, Kaveh 2014). To increase the processing velocity and accuracy of networks, the input data were normalized at boundary of [0, 1].

RESULTS AND DISCUSSION

Plotting the logarithm of *MR* values versus the drying time gave the values of D_{eff} for different temperatures together with regression coefficient of determination (R^2). From the results, D_{eff} increased with the increasing drying air temperature. The values of D_{eff} ranged from 10^{-9} to 10^{-11} m^2/s (Vega-Gálvez et al. 2012). The values of D_{eff} for terebinth ranged from 1.1×10^{-10} to 1.26×10^{-10} m^2/s. Several investigations carried out on fruits and vegetables under similar temperature and velocity conditions showed D_{eff} values to lie between $3.22–15.3 \times 10^{-9}$ m^2/s for apple (Vega-Gálvez et al. 2012), $1.72–3.31 \times 10^{-11}$ m^2/s for rape seed (Duc et al. 2011), 8.21×10^{-10} to 2.61×10^{-9} m^2/s for castor oil seeds (Perea-Flores et al. 2012). The following model is proposed to describe D_{eff} of the terebinth fruit under fluidized bed dryer:

$$D_{eff} = 0.55 \times 10^{-11} v + 0.22 \times 10^{-12} T_c + -0.39 \times 10^{-9}$$
$$R^2 = 0.9692 \quad (13)$$

where:
v – airflow velocity (m/s)
T_c – air temperature (°C)

Two networks of FFNN and CFNN were applied to map between inputs and outputs of patterns. Different compositions of threshold functions were tested in layers. Several topologies were used and the best results were recommended from each training algorithm, threshold function and network (Table 2). The best results belonged to CFNN network, TANSIG threshold function and 2-3-1 topology. This composition produced $MSE = 0.000004$, $R^2 = 0.9932$, $MAE = 3 \times 10^{-11}$ and $STD_{MAE} = 6.15$ converged in 12 epochs. The R^2 of optimized ANN is plotted in Fig. 4. This trend is identical to those reported in studies on agriculture and food plants (Aghbashlo et al. 2011; Amiri Chayjan et al. 2012).

Fig. 4 indicates the desired output values versus the predicted values on a plot of moisture diffusivity for kinetics analyses of fluidized bed drying of terebinth fruit using the optimized ANN.

It was observed that shrinkage of terebinth fruit increased with an increase in the temperature and air velocity. Max. shrinkage value (72.2%) occurred at air temperature of 80°C and air velocity of 4.43 m/s. Min. shrinkage (60.92%) was obtained at air temperature of 40°C and air velocity of 0.81m/s. Shrinkage percentage (S_b) of terebinth fruit under different bed conditions is presented in the following model:

$$S_b = 0.37v + 0.01T_c + 0.60 \times 10^{-2} T_c v + 1.02$$
$$R^2 = 0.9684 \quad (14)$$

where:
T_c – air temperature
v – airflow velocity (m/s)

For all bed conditions, the SEC decreased as drying air temperature was increased. Max. value of *SEC* (1246.4 MJ/kg) was obtained at fluid bed condition with air velocity of 4.43 m/s and air temperature of 40°C, while the min. value of *EC* (130.2 MJ/kg) was calculated at fix bed condition with air velocity of 0.81 m/s and air temperature of 80°C. Specific energy consumption of terebinth fruit under different bed conditions is presented in the following model:

$$SEC = 28.05 \times 10^3 v + 12.49 \times 10^2 T_c + 4.55 \times 10^2 T_c v + 76.99 \times 10^3$$
$$R^2 = 0.9853 \quad (15)$$

where:
T_c – air temperature
v – airflow velocity (m/s)

Two strategies of similar and various threshold functions for all layers were utilized to study the effect of different threshold functions on FFNN and CFNN outputs (Table 2). Both strategies, as well as learning algorithms of LM and BR, were used for training of FFNN and CFNN networks. Several topologies were selected as the best results from each threshold function, training algorithm and network.

The best results for FFNN for shrinkage (Table 2) belonged to 2-3-3-1 topology and TANSIG-LOGSIG-TANSIG threshold function with LM algorithm in the first strategy. This structure generated

doi: 10.17221/56/2013-RAE

Table 2. Best selected topologies including training algorithm, different layers and neurons for FFNN and CFNN for effective moisture diffusivity, shrinkage and specific energy consumption

Network	Training algorithm	Threshold function	No. of layers and neurons	*MSE*	R^2	*MAE*	STD_{MAE}	Epoch
Effective moisture diffusivity								
FFNN	LM	TANSIG-PURELIN-TANSIG	2-3-2-1	0.0009	0.9601	6.17×10^{-11}	8.11	19
		TANSIG	2-3-1	0.00001	0.9876	4.95×10^{-11}	10.57	10
	BR	LOGSIG-PURELIN-TANSIG	2-3-3-1	0.00334	0.9501	6.99×10^{-11}	12.25	14
		TANSIG	2-5-1	0.00221	0.9514	6.44×10^{-11}	9.57	39
CFNN	LM	TANSIG-LOGSIG-TANSIG	2-3-3-1	0.00012	0.9872	3.48×10^{-11}	7.1	10
		TANSIG	2-3-1	0.000004	0.9932	3.00×10^{-11}	6.15	12
	BR	TANSIG-LOGSIG-TANSIG	2-4-3-1	0.0013	0.9765	4.87×10^{-11}	8.11	17
		TANSIG	2-5-1	0.0007	0.9802	4.09×10^{-11}	8.39	19
Shrinkage								
FFNN	LM	TANSIG-LOGSIG-TANSIG	2-3-3-1	0.00118	0.9774	0.242	0.90	10
		LOGSIG-PURELIN-TANSIG	2-3-2-1	0.00189	0.9769	0.381	0.64	105
	BR	TANSIG	2-2-4-1	0.00661	0.9548	0.520	0.85	14
		TANSIG	2-5-1	0.00216	0.9705	0.391	0.21	19
CFNN	LM	TANSIG-PURELIN-TANSIG	2-3-4-1	0.00087	0.9887	0.412	0.74	8
		TANSIG	2-4-1	0.00001	0.9917	0.136	0.64	11
	BR	TANSIG- TANSIG-PURELIN	2-4-3-1	0.00122	0.9806	0.322	0.57	9
		TANSIG	2-5-1	0.00176	0.9761	0.378	0.65	10
Specific energy consumption								
FFNN	LM	TANSIG	2-4-1	0.00114	0.9827	42.57	8.07	33
		PURELIN -LOGSIG-TANSIG	2-3-4-1	0.00401	0.9734	44.43	7.66	11
	BR	TANSIG	2-2-3-1	0.00334	0.9780	45.31	8.97	23
		TANSIG	2-5-1	0.00516	0.9667	47.54	11.12	113
CFNN	LM	TANSIG	2-2-1	0.00047	0.9855	41.32	9.46	6
		TANSIG-PURELIN-TANSIG	2-4-3-1	0.00351	0.9769	46.95	11.54	11
	BR	TANSIG	3-3-4-1	0.00654	0.9221	59.87	16.7	90
		TANSIG	2-4-1	0.02114	0.8885	61.83	15.89	10

FFNN – Feed Forward Neural Network; CFNN – Cascade Forward Neural Network; LM – Levenberg-Marquardt; BR – Bayesian regulation; *MSE* – mean square error, R^2 – determination coefficient; *MAE* – mean absolute error, STD_{MAE} – Standard deviation of mean absolute error; Epoch – learning cycle

MSE = 0.00118, R^2 = 0.9774 and *MAE* = 0.242 converged in 10 epochs. The best results for FFNN for specific energy consumption (Table 2) belonged to 2-3-4-1 topology and PURELIN-LOGSIG-TANSIG threshold function with LM algorithm in the first strategy. This structure generated *MSE* = 0.00401, R^2 = 0.9734 and *MAE* = 44.43 converged in 11 epochs.

The best results for CFNN for shrinkage belonged to topology of 2-4-1 with LM algorithm, threshold function of TANSIG and the first strategy. This composition output was *MSE* = 0.00001, *MAE* = 0.136 and R^2 = 0.9917 at 11 training epochs. Also, the best results for CFNN for specific energy consumption belonged to topology of

doi: 10.17221/56/2013-RAE

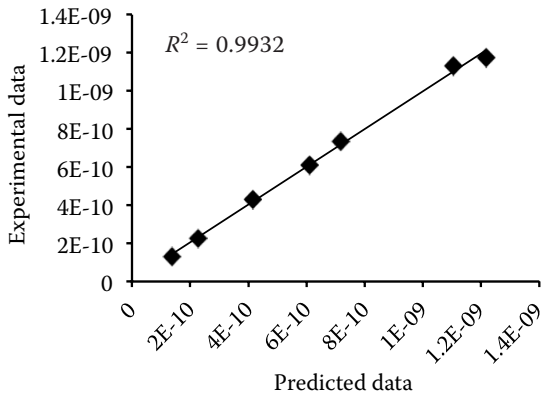

Fig. 4. Predicted values of effective moisture diffusivity using artificial neural networks versus experimental values for testing data set

2-2-1 with LM algorithm, threshold function of TANSIG and the first strategy. This composition output was *MSE* = 0.00047, *MAE* = 41.32 and R^2 = 0.9855 at 11 training epochs.

Fig. 5 compares the desired output values with the predicted values on a plot of shrinkage and energy consumption for kinetics analyses of fluidized bed drying of terebinth fruit using the optimal static ANN.

Fig. 6 illustrates the drying rate versus drying time at drying temperatures of 40, 50, 60, 70 and 80°C. After sample heating at the initial period, the drying rate reached its max. value and then the product dried at the falling rate period. Mass transfer takes place initially at the sample surface and loses relevance at subsequent stages. After surface drying, the moisture diffusion process becomes the most important factor. However, three different drying periods observed during the experiment performed at 40°C is an exception to such tendency. An initial heating period was followed by a constant rate period, and finally by the falling rate period.

These experimental results are similar to some others published in literature, relating to drying experiments concerning vegetables and agricultural products; for instance grape (Ruiz Celma et al. 2009), poplar sawdust (Chen et al. 2012), barley (Markowski et al. 2010) and rice (Zielinska, Cenkowski 2012).

In this paper, an artificial neural networks (ANN) model with one and two hidden layers for the determination of drying behaviours, such as MR and DR, were developed. In the model, MR and DR are the outputs, whereas air temperature, velocity and time are the inputs. In this study, different ANN topologies were tested to predict the moisture ratio of terebinth fruits based on the drying time, air temperature and air velocity. The training error was associated with different hidden layers and ANN configurations. It is evident that the learning ability of the two-hidden layer networks was significantly higher than that for one-hidden layer. This showed that increasing the hidden layer number increased the learning capability of the networks. Also, the neuron number in the hidden layers had a significant role in learning performance of an ANN model. The neuron numbers within hidden layers can be varied based on the problem complexity and data set. However, training of an ANN topology with the best performance is the key to build an ANN structure to be able to predict outputs precisely.

Two aforementioned strategies were also used to predict the *DR* and *MR* (Table 3). Both strategies, as well as the learning algorithms of LM and BR,

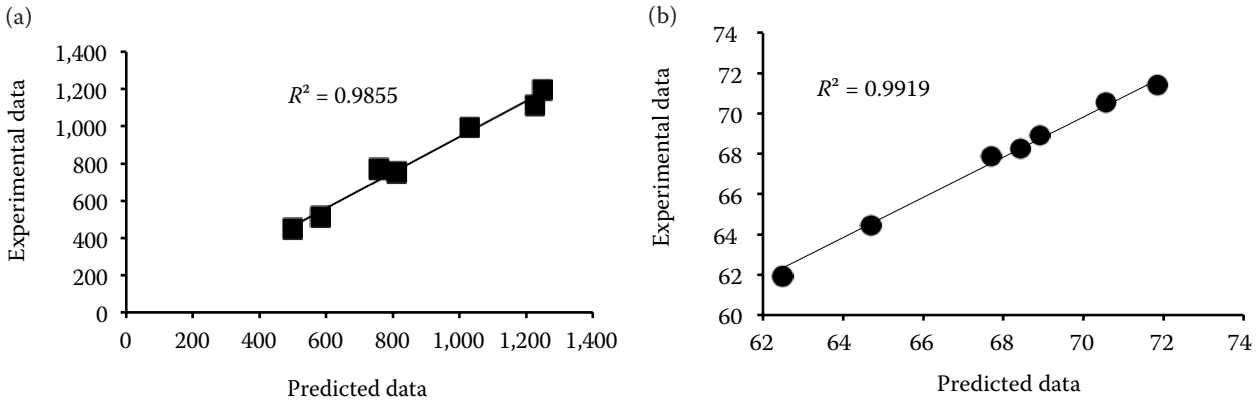

Fig. 5. Predicted values of (a) energy consumption and (b) shrinkage using artificial neural networks versus experimental values for testing data set

doi: 10.17221/56/2013-RAE

(a)

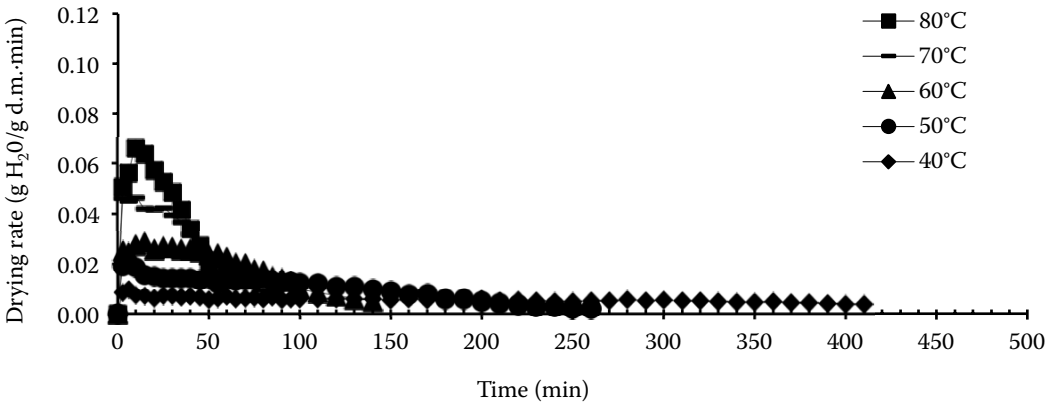

(b)

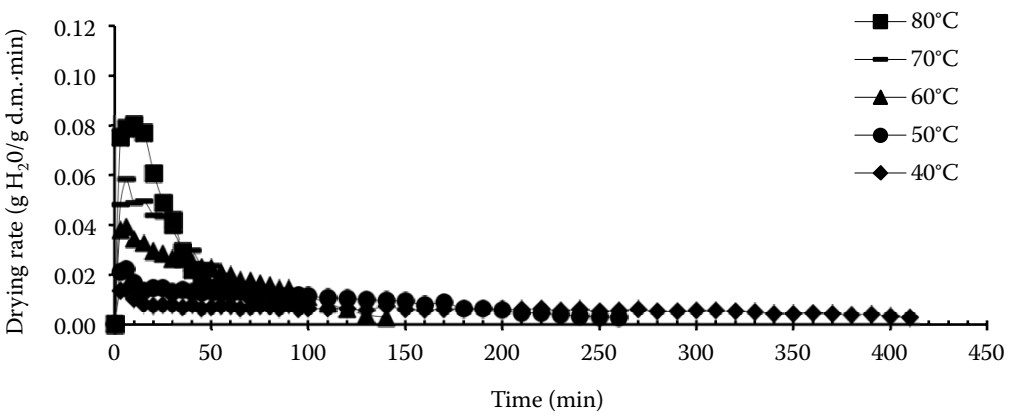

(c)

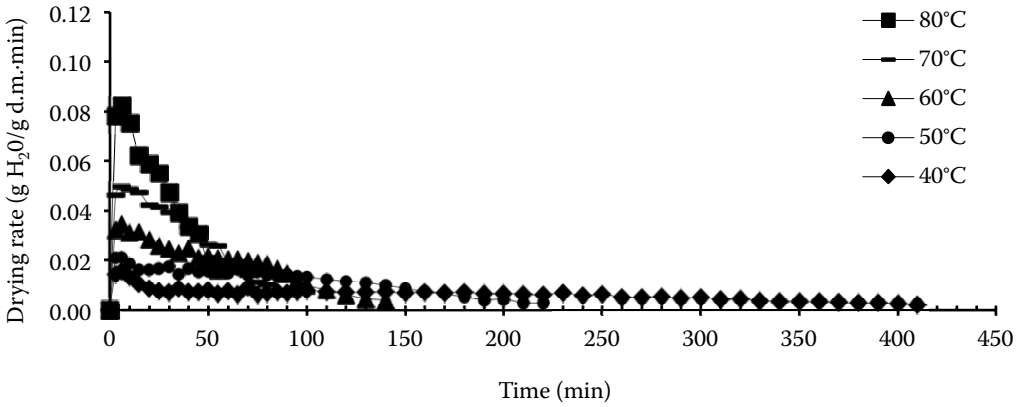

(d)

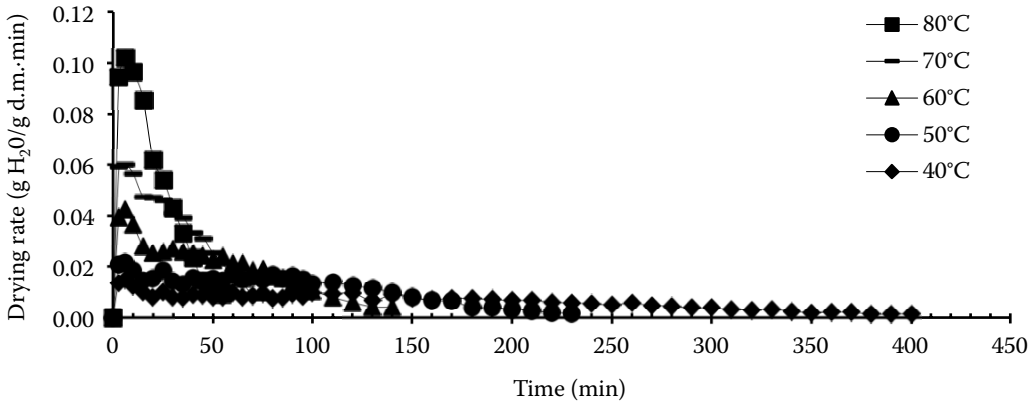

doi: 10.17221/56/2013-RAE

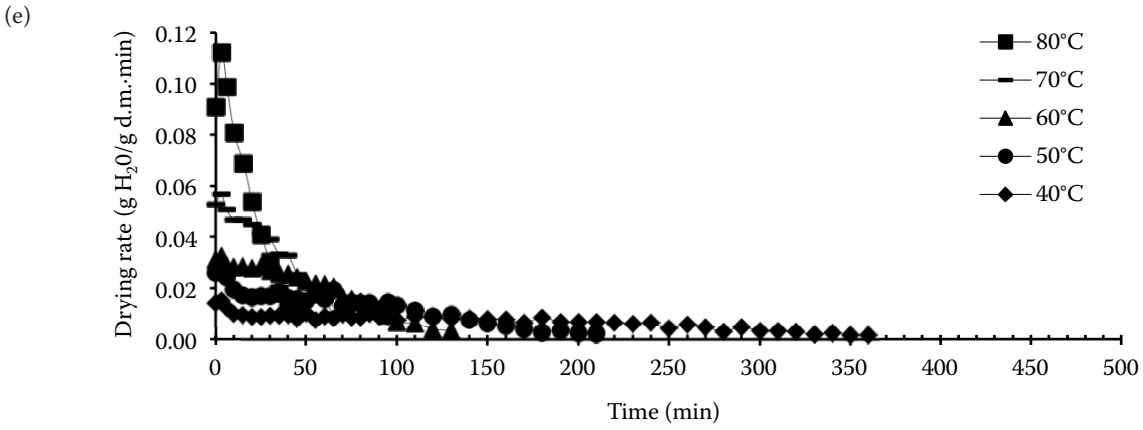

Fig. 6. Drying rates versus drying time (min) at different temperatures and air velocities: (a) fix bed (0.81 m/s), (b) fix bed (1.35 m/s), (c) semi fluid bed (2.08 m/s), (d) fluid bed (3.34 m/s) and (e) fluid bed (4.43 m/s)

were used for training of FFNN and CFNN networks. Several topologies were selected as the best results from each network, training algorithm and threshold functions.

The best results for FFNN for *DR* and *MR* belonged to 3-4-3-2 topology and LOGSIG-TANSIG-PURELIN threshold function with LM algorithm in the first strategy (Table 3). This structure generated *MSE* = 0.00047, R^2 = 0.9670 for *DR*, R^2 = 0.9965 for *MR*, *MAE* = 0.0015 for DR and *MAE* = 0.0142 for MR and converged in 75 epochs. Also, the best results for CFNN for *DR* and *MR* consumption belonged to topology of 3-3-3-2 with LM algorithm, threshold function of TANSIG and the first strategy. This composition output was *MSE* = 0.00014, *MAE* = 0.0014 for *DR*, *MAE* = 0.0134 for *MR*, R^2 = 0.9730 for *DR* and 0.9965 for MR at 275 training epochs.

Fig. 7 compares the predicted values with the desired output values on a plot of drying rate and moisture ratio for kinetics analyses of fluidized bed drying of terebinth fruit using the optimal static ANN. These results imply that the designed ANN model was properly capable of learning the relationship between the input and output parameters. These results also confirm that unlike mathematical models, a properly trained neural network was able to produce simultaneously more than one output (Table 3). The optimized ANN model provided satisfactory results over the whole set of values for all of the dependent variables.

Table 3. Best selected topologies including training algorithm, different layers and neurons for FFNN and CFNN for *DR* and *MR*

Network	Training algorithm	Threshold function	No. of layers and neurons	*MSE*	*MAE*		R^2		Epoch
					(*DR*)	(*MR*)	(*DR*)	(*MR*)	
FFNN	LM	TANSIG-LOGSIG-PURELIN	3-3-3-2	0.00069	0.0016	0.0161	0.9669	0.9951	103
		LOGSIG-TANSIG-PURELIN	3-4-3-2	0.00047	0.0015	0.0142	0.9670	0.9965	75
	BR	TANSIG	3-3-2-2	0.00175	0.0017	0.0181	0.9656	0.9940	198
		TANSIG-PURELIN-TANSIG	3-4-3-2	0.00230	0.0021	0.0180	0.9628	0.9940	101
CFNN	LM	TANSIG	3-3-3-2	0.00014	0.0014	0.0121	0.9730	0.9965	275
		TANSIG-TANSIG-PURELIN	3-2-3-2	0.00042	0.0014	0.0134	0.9729	0.9956	317
	BR	TANSIG	3-4-3-2	0.00059	0.0015	0.0144	0.9650	0.9960	65
		TANSIG-LOGSIG-TANSIG	3-3-3-2	0.00204	0.0017	0.0176	0.9696	0.9933	26

DR – Drying rate, *MR* – Moisture ratio; for abbreviations see Table 2

doi: 10.17221/56/2013-RAE

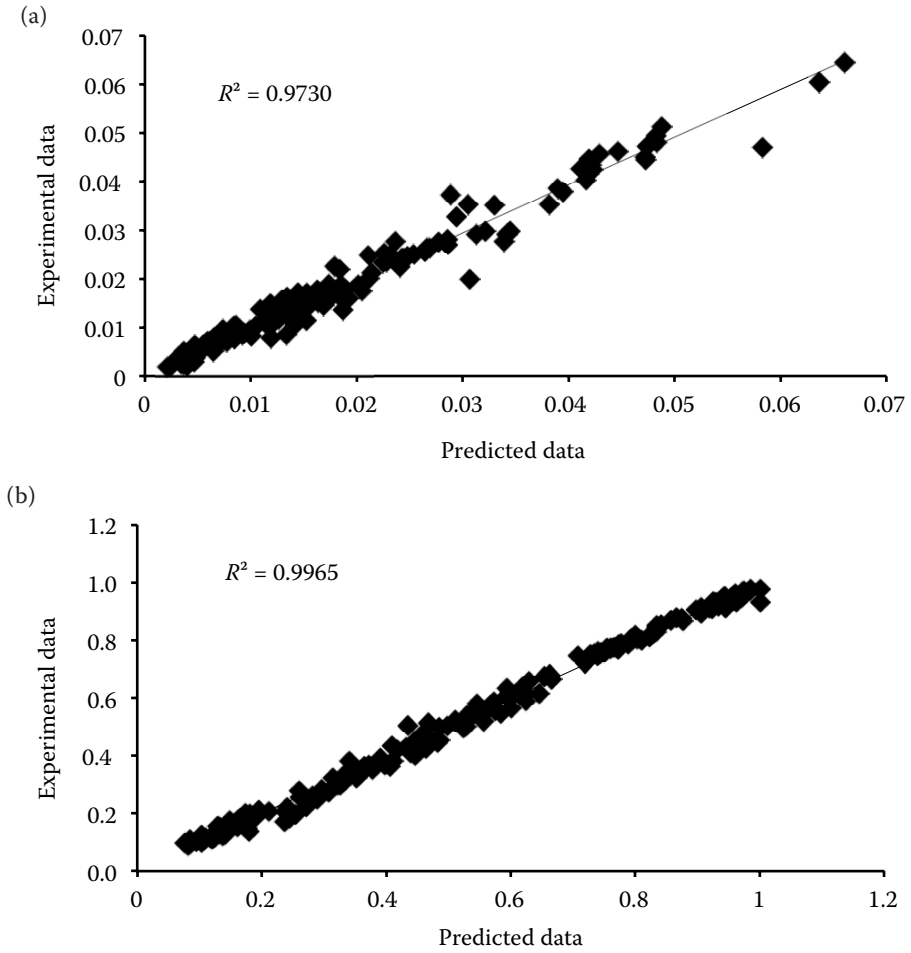

Fig. 7. Predicted values of (a) drying rate and (b) moisture ratio using artificial neural networks versus experimental values for testing data set

CONCLUSION

In this paper, terebinth fruit drying behaviour at different air velocity of 0.81, 1.35, 2.08, 3.35 and 4.43 m/s and air temperatures of 40, 50, 60, 70 and 80°C was studied. The best results for D_{eff} perdition by ANN approach belonged to CFNN network, TANSIG threshold function and 2-3-1 topology. This composition produced MSE = 0.000004, R^2 = 0.9932, $MAE = 3 \times 10^{-11}$ and STD_{MAE} = 6.15 converged in 12 epochs. The best results for CFNN for DR and MR consumption belonged to topology of 3-3-3-2 with LM algorithm, threshold function of TANSIG and the first strategy. This composition output was MSE = 0.00014, MAE = 0.0014 for DR, MAE = 0.0134 for MR, R^2 = 0.9730 for DR, R^2 = 0.9965 for MR at 275 training epochs.

References

Aghbashlo M., Kianmehr M.H., Arabhosseini A., Nazghelichi T. (2011): Modelling the carrot thin-layer drying in a semi-industrial continuous band dryer. Czech Journal of Food Sciences, 28: 531–537.

Alibas I. (2007): Energy consumption and colour characteristics of nettle leaves during microwave, vacuum and convective drying. Biosystems Engineering, 96: 495–502.

Amiri Chayjan R., Esna-Ashari M. (2010): Comparison between artificial neural networks and mathematical models for estimating equilibrium moisture content in raisin. Agricultural Engineering International: CIGR Journal, 12: 158–166.

Amiri Chayjan R., Salari K., Barikloo H. (2012): Modeling moisture diffusivity of pomegranate seed cultivars under fixed, semi fluidized and fluidized bed using mathematical and neural network methods. Acta Scitiuarum Polonorom Technologia Alimentaria, 11: 137–149.

Amiri Chayjan R., Kaveh M. (2014): Physical parameters and kinetic modeling of fix and fluid bed drying of terebinth seeds. Journal of Food Processing and Preservation, 38: 1307–1320.

Bala B.K., Ashraf M.A., Uddin M.A. Janjai S. (2005): Experimental and neural network prediction of the performance of the solar tunnel dryer for drying of jackfruit bulbs and jackfruit leather. Journal of Food Process Engineering, 28: 552–566.

doi: 10.17221/56/2013-RAE

Cakmak G., Yildiz C. (2011): The prediction of seedy grape drying rate using a neural network method. Computers and Electronics in Agriculture, 75: 132–138.

Chen D., Zheng Y., Zhu X. (2012): Determination of effective moisture diffusivity and drying kinetics for poplar sawdust by thermogravimetric analysis under isothermal condition. Bioresource Technology, 107: 451–455.

Demuth H., Beale M., Hagan M. (2007): Neural network toolbox 5. Natick, The MathWorks.

Duc L.A., Han J.W., Keum D.H. (2011): Thin layer drying characteristics of rape seed (*Brassica napus* L.). Journal of Stored Products Research, 47: 32–38.

Hashemi G., Mowla D., Kazemeini M. (2009): Moisture diffusivity and shrinkage of broad beans during bulk drying in an inert medium fluidized bed dryer assisted by dielectric heating. Journal of Food Engineering, 92: 331–338.

Keeratipibul S., Phewpan A., Lursinsap C. (2011): Prediction of coliforms and *Escherichia coli* on tomato fruits and lettuce leaves after sanitizing by using artificial neural networks. LWT-Food Science and Technology, 44*:* 130–138.

Lertworasirikul S., Tipsuwan Y. (2008): Moisture content and water activity prediction of semi-finished cassava crackers from drying process with artificial neural network. Journal of Food Engineering, 84*:* 65–74.

Markowski M., Białobrzewski I., Modrzewska A. (2010): Kinetics of spouted-bed drying of barley: Diffusivities for sphere and ellipsoi. Journal of Food Engineering, 96: 380–387.

Mayor L., Sereno A.M. (2004): Modeling shrinkage during convective drying of food material: a review. Journal of Food Engineering, 18: 373–386.

Movagharnejad K., Nikzad M. (2007): Modelling of tomato drying using artificial neural network. Computers and Electronics in Agriculture, 59: 78–85.

Nazghelichi T., Aghbashlo M., Kianmehr M.H. (2011): Optimization of an artificial neural network topology using coupled response surface methodology and genetic algorithm for fluidized bed drying. Computers and Electronics in Agriculture, 75*:* 84–91.

Niamnuy C., Nachaisin M., Poomsaad N., Devahastin S. (2012): Kinetic modelling of drying and conversion/degradation of isoflavones during infrared drying of soybean. Food Chemistry, 133: 946–952.

Perea-Flores M.J., Garibay-Febles V., Chanona-Pérez J.J., Calderón-Domínguez G., Méndez-Méndez J.V., Palacios-González E., Gutiérrez-López G.F. (2012): Mathematical modelling of castor oil seeds (*Ricinus communis*) drying kinetics in fluidized bed at high temperatures. Industrial Crops and Products, 38*:* 64–71.

Ruiz Celma A., López-Rodríguez F., Cuadros Blázquez F. (2009): Experimental modelling of infrared drying of industrial grape by-products. Food and Bioproducts Processing, 87: 247–253.

Vega-Gálvez A., Ah-Hen K., Chacana M., Vergara J., Martínez-Monzó J., García-Segovia P., Lemus-Mondaca R., Di Scala K. (2012): Effect of temperature and air velocity on drying kinetics, antioxidant capacity, total phenolic content, colour, texture and microstructure of apple (var. Granny Smith) slices. Food Chemistry, 132: 51–59.

Zielinska M., Cenkowski S. (2012): Superheated steam drying characteristic and moisture diffusivity of distillers' wet grains and condensed distillers' solubles. Journal of Food Engineering, 109: 627–634.

Received for publication July 30, 2013
Accepted after corrections January 29, 2014

Corresponding author:

R. Amiri Chayjan, Bu-Ali Sina University, Faculty of Agriculture, Department of Biosystems Engineering, 6517833131, Hamedan, Iran
phone: + 98 811 4424 366; fax: + 98 811 4224 012; e-mail: amirireza@basu.ac.ir